

Heterozygous Germline Mutations in the p53 Homolog p63 Are the Cause of EEC Syndrome

Jacopo Celli,^{1,14} Pascal Duijf,^{1,14} Ben C. J. Hamel,¹ Michael Bamshad,² Bridget Kramer,² Arie P. T. Smits,¹ Ruth Newbury-Ecob,³ Raoul C. M. Hennekam,⁴ Griet Van Buggenhout,⁵ Arie van Haeringen,⁶ C. Geoffrey Woods,⁷ Anthonie J. van Essen,⁸ Rob de Waal,⁹ Gert Vriend,¹⁰ Daniel A. Haber,¹¹ Annie Yang,¹² Frank McKeon,¹² Han G. Brunner,¹ and Hans van Bokhoven^{1,13}

¹Department of Human Genetics 417
University Hospital Nijmegen
Box 9101

6500 HB Nijmegen
The Netherlands

²Department of Pediatrics
University of Utah Health Sciences Center
and Shriners Hospitals for Children
Intermountain Unit
Salt Lake City, Utah 84112

³The United Bristol Healthcare
NHS Trust Clinical Genetics Service
Bristol Royal Hospital for Sick Children
Bristol, BS2 8BJ, United Kingdom

⁴Institute for Human Genetics
Academic Medical Centre
1105 AZ Amsterdam, The Netherlands

⁵Center for Human Genetics
University Hospital Gasthuisberg
3000 Leuven, Belgium

⁶Department of Clinical Genetics
Leiden University Medical Centre
2333 SA Leiden, The Netherlands

⁷Department of Clinical Genetics
St. James's University Hospital
Leeds, LS9 7TF England

⁸Department of Medical Genetics
University of Groningen
9713 AW Groningen, The Netherlands

⁹Department of Pathology
University Hospital Nijmegen
6500 HB Nijmegen, The Netherlands

¹⁰CMBI
University of Nijmegen
6500 GL Nijmegen, The Netherlands

¹¹Massachusetts General Hospital Cancer Center
Charlestown, Massachusetts 02129

¹²Department of Cell Biology
Harvard Medical School
Boston, Massachusetts 02115

Summary

EEC syndrome is an autosomal dominant disorder characterized by ectrodactyly, ectodermal dysplasia, and facial clefts. We have mapped the genetic defect

in several EEC syndrome families to a region of chromosome 3q27 previously implicated in the EEC-like disorder, limb mammary syndrome (LMS). Analysis of the *p63* gene, a homolog of *p53* located in the critical LMS/EEC interval, revealed heterozygous mutations in nine unrelated EEC families. Eight mutations result in amino acid substitutions that are predicted to abolish the DNA binding capacity of p63. The ninth is a frameshift mutation that affects the p63 α , but not p63 β and p63 γ isoforms. Transactivation studies with these mutant p63 isoforms provide a molecular explanation for the dominant character of p63 mutations in EEC syndrome.

Introduction

The central reduction defect of the hands and feet known as ectrodactyly, split hand/split foot malformation (SHFM), or lobster-claw, occurs in approximately 1 in 18,000 newborns (Czeizel et al., 1993; Evans et al., 1994). The etiology of this condition is unknown, but several genetic factors may be involved. Based on linkage studies and the analysis of chromosomal abnormalities, three loci have been identified in humans: *SHFM1* on 7q21.3-q22.1 (Scherer et al., 1994; Crackower et al., 1996), *SHFM2* on Xq26 (Ahmad et al., 1987), and *SHFM3* on 10q24-q25 (Nunes et al., 1995; Raas-Rothschild et al., 1996). In almost 40% of the cases, ectrodactyly is associated with other anomalies (Czeizel et al., 1993; Evans et al., 1994). A well-known example is the EEC syndrome, which comprises Ectrodactyly, Ectodermal dysplasia, and Cleft lip with or without cleft palate. EEC syndrome has an autosomal dominant mode of inheritance with highly variable expression and reduced penetrance. Ectodermal dysplasia in the EEC syndrome affects the skin, hair, nails, and teeth (Roelfsema and Cobben, 1996). Other symptoms are lacrimal duct abnormalities, urogenital problems, conductive hearing loss, facial dysmorphism, chronic/recurrent respiratory infections, and developmental delay (Gorlin et al., 1990). A locus for EEC syndrome on chromosome 19 was identified in a family from the Netherlands with EEC syndrome and urogenital defects (O'Quinn et al., 1998). We recently mapped the genetic defect in another large Dutch family with an EEC-like phenotype to chromosome 3q27 (van Bokhoven et al., 1999). The condition in this family could be distinguished clinically from EEC syndrome and was denoted limb mammary syndrome (LMS).

Here we report the construction of a physical map from a 3 cM region containing the causative gene for LMS. Linkage analysis revealed that the genetic defect in several EEC syndrome families colocalizes with the LMS locus. This observation suggested that these disorders are allelic. YAC clones covering the EEC/LMS critical region were used to map ESTs and the positional candidate genes *SOX2*, *DVL3*, *LPP*, *Chordin*, and *p63*. In addition to several ESTs, only *p63* was found to exactly map within this region. The *p63* gene (Osada et

¹³To whom correspondence should be addressed (e-mail: h.vanbokhoven@antrg.azn.nl).

¹⁴These authors contributed equally to this work.

Table 1. Linkage Analysis in Families with EEC Syndrome

Family	Locus	Z _{max} at $\theta = 0$	Flanking Markers (Proximal-Distal)
LMS	D3S3530	12.01	D3S1580-D3S1314
Ams-1	D3S3530	4.53	ND ^a -D3S1314
	D19S49	4.06	D19S894-D19S416
SLC-1	D3S3530	0.86	ND ^a
SLC-2	D3S3530	1.76	ND ^a
Bri-1	D3S1294	1.81	D3S3530-3qter
Leu-1	D3S3530	0.88	ND ^a

Linkage analysis in the EEC syndrome families was performed with markers from the critical region that was defined previously for LMS (van Bokhoven et al., 1999). Reconstructing haplotypes identified flanking markers for the EEC syndrome families. Note that family Ams-1 shows significant LOD scores for two loci. The chromosome 19 locus was found previously by O'Quinn et al. (1998).

^aFor these families no recombinations were detected in the region around 3q27.

al., 1998; Senoo et al., 1998; Trink et al., 1998; Yang et al., 1998), a homolog of the archetypal tumor suppressor gene *p53*, is abundantly expressed in proliferating basal cells of epithelial layers in the epidermis (Yang et al., 1998). In keeping with this expression pattern are the phenotypes of the recently reported *p63* knockout mice (Yang et al., 1999; Mills et al., 1999). *p63*-deficient mice lack all squamous epithelia and their derivatives, including hair, whiskers, teeth, as well as the mammary, lacrimal, and salivary glands. Particularly striking are severe limb truncations with forelimbs showing a complete absence of the phalanges and carpals, and variable defects of ulnae and radiae and hindlimbs that are lacking altogether. Subsequent analysis of the *p63* gene revealed heterozygous mutations in nine unrelated patients with EEC syndrome. The *p63* mutations act in a dominant fashion in humans, giving rise to a phenotype that resembles that of *p63* knockout mice.

Results

Linkage Analysis in EEC Families

To investigate the possibility of allelism with LMS, polymorphic markers from the 3q27 region were used for a linkage analysis in five families with EEC syndrome. Positive LOD scores were obtained with markers from within the LMS interval for each of these families (Table 1). The added Z_{max} across these families is 8.03 at marker D3S3530 at a recombination fraction $\theta = 0$. Recombination events were observed between markers that define the LMS interval, D3S1580 and D3S1314, and the disease locus, indicating that these five EEC syndrome families map to the same 3 cM region of 3q27 that was previously found for the LMS family (van Bokhoven et al., 1999). This colocalization and the overlapping clinical features of these disorders strongly suggest that the same gene is involved in both EEC and LMS. If so, the critical region for EEC/LMS was reduced to a 2.3 cM interval by a recombination event between marker D3S3530 and the genetic defect in EEC family Bri-1 (64:1 odds).

Physical Mapping of the LMS Critical Region

By using the Whitehead STS-based map of the human genome, YAC clones were selected that each should contain several STSs from the region around D3S1580 and D3S1314. The size and integrity of the YACs was determined by pulsed field gel electrophoresis and Southern blots probed with total human DNA (data not shown). PCR was then performed to map STSs on the YACs. This approach allowed us to place the YACs into a contig covering the critical region for LMS/EEC syndrome (Figure 1). Five STSs within this region were derived from expressed sequences (ESTs): A004N18, WI-6145, WI-19957, STSG1588, and SGC33716. According to the Unigene database, each of these five ESTs represents a cluster of 2 to 65 cDNA clones derived from

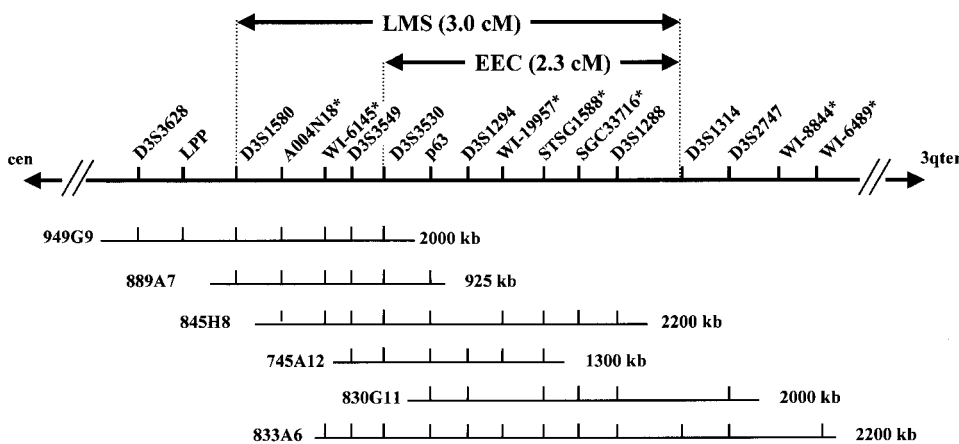


Figure 1. Physical Map of the Region Containing the Gene for EEC/LMS Syndrome

Genetic intervals for LMS and EEC syndrome are shown at top. The physical map underneath shows the approximate positions of genetic markers, ESTs (indicated by asterisks), and the *LPP* and *p63* genes. The order of genetic markers was deduced from genetic maps (Dib et al., 1996), and confirmed by mapping of these markers to partially overlapping YAC clones from the 3q27 region. The vertical lines at the YAC clones indicate the presence of a STS/EST as determined by PCR. YAC clones are from the CEPH megabase YAC library. Five ESTs map to the LMS region and three map to the combined EEC/LMS region. The *p63* gene is the only full-length cDNA that maps to the LMS/EEC critical region.

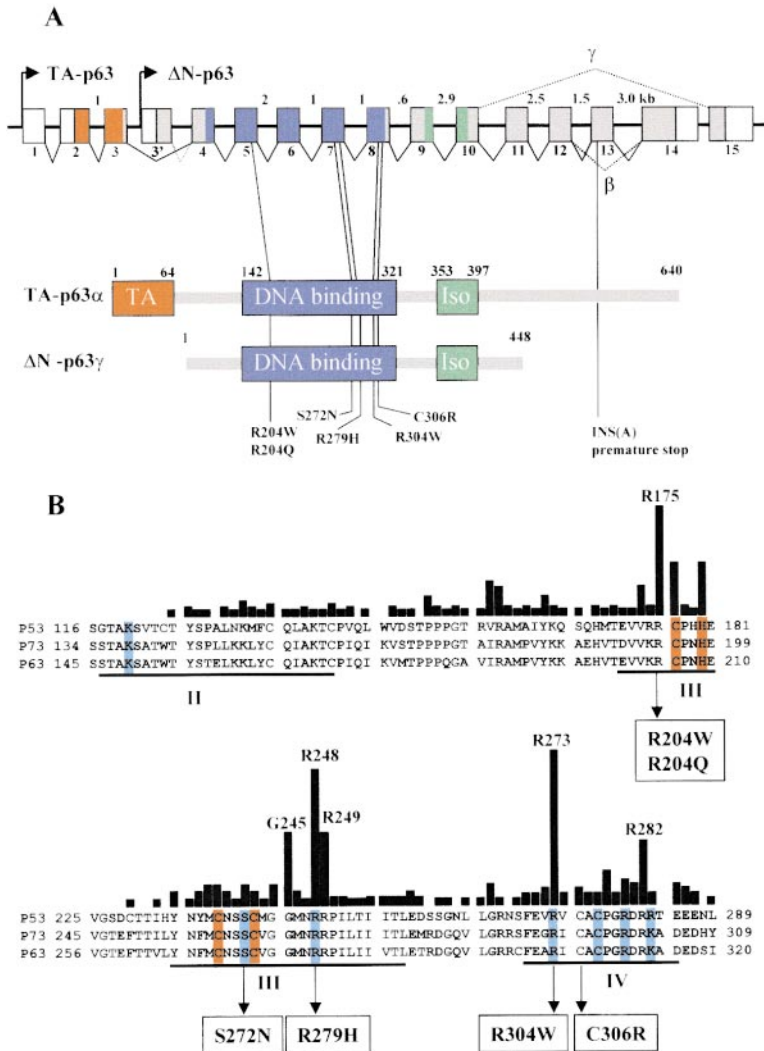


Figure 2. Schematic Representation of the Human *p63* Gene and Position of Mutations Found in EEC Syndrome Patients

(A) Intron-exon structure of the *p63* gene showing the two transcriptional start sites and the various splicing events leading to the 6 known isoforms of *p63* (Yang et al., 1998). Initiation of transcription in exon 1 produces the TA-isotypes, containing the transactivation (TA) domain, while initiation in exon 3' gives rise to the ΔN-isotypes without the TA domain. The splicing events that produce the α isotypes are indicated with solid lines; splicing events that produce the β and γ isotypes are indicated with dotted lines. Protein domains are shown for the TA-p63α and ΔN-p63γ isotypes. The open reading frame is indicated in gray; conserved protein domains are highlighted with colors: red, transactivation domain; blue, DNA-binding domain; green, isomerization domain. All missense mutations are located in the DNA-binding domain, which is contained in all 6 *p63* isotypes. The frameshift mutation [INS(A)] located in exon 13 is predicted to produce truncated α isotypes, whereas the β and γ isotypes are left unaffected.

(B) Amino acid sequence comparison of the DNA-binding domain of human p53, p63, and p73. The highly conserved domains II to IV that were identified by Cho et al. (1994) are underlined. Blue shading depicts amino acids that directly contact the DNA, and the red colors indicate the Zn-binding amino acids. The black bars indicate the relative frequency of mutations that are found at a particular amino acid of p53 from human tumor material (Hollstein et al., 1991; Hainaut et al., 1998). All amino acid substitutions that are found in the *p63* gene of EEC syndrome patients are located in the conserved domains, and often affect residues that bind to DNA or residues that are frequently mutated in p53.

a variety of cDNA libraries. We checked by PCR the localization of 5 known genes (*LPP*, *Chordin*, *DVL3*, *SOX2*, and *p63*) on our YAC panel. *Chordin*, *SOX2*, and *DVL3* were negative for all YACs, whereas PCR fragments of expected sizes were obtained in the reaction with total human DNA. *LPP* was positive only for YAC 949G9, indicating that this gene is just outside the LMS/EEC critical region. However, it cannot be excluded that part of the *LPP* gene or of its regulatory elements is within the LMS/EEC region. We therefore sequenced all coding exons and flanking intron sequences of the *LPP* gene in one LMS patient. Except for one intron polymorphism, no deviations from the reported sequences were detected. Finally, PCR amplification of part of exon 14 of the *p63* gene revealed that this gene maps precisely within the LMS critical region. This localization, in combination with the high expression level of *p63* in epidermal cells and the phenotype of the recently reported *p63* knockout mice (Yang et al., 1999; Mills et al., 1999), make this gene a likely candidate for LMS and EEC syndrome.

p63 Mutation Analysis

The *p63* gene encodes multiple isoforms by two transcription initiation sites and extensive alternative splicing (Yang et al., 1998; Figure 2A). Since only the cDNA sequences of the human *p63* gene were known, we set out to resolve the genomic structure via an exon bridging technique. Exon-specific primers were designed based on the proposed *p63* gene structure (Yang et al., 1998). By long-range PCR with YAC DNA as template, we were able to amplify most of the introns of this gene (Figure 2A). The splice sites and flanking intron sequences of the PCR fragments were determined. These data allowed us to design intron-specific primers suitable for amplification of exons 5 to 14. The resulting PCR fragments obtained from 25 unrelated EEC syndrome patients and a patient from the LMS family were analyzed for mutations by direct sequencing. A total of nine heterozygous nucleotide changes were detected in EEC syndrome patients (Figure 2). The arginine at position 204 (numbering based on the TA-p63α isotype) was found to be mutated in four unrelated patients, with three of these

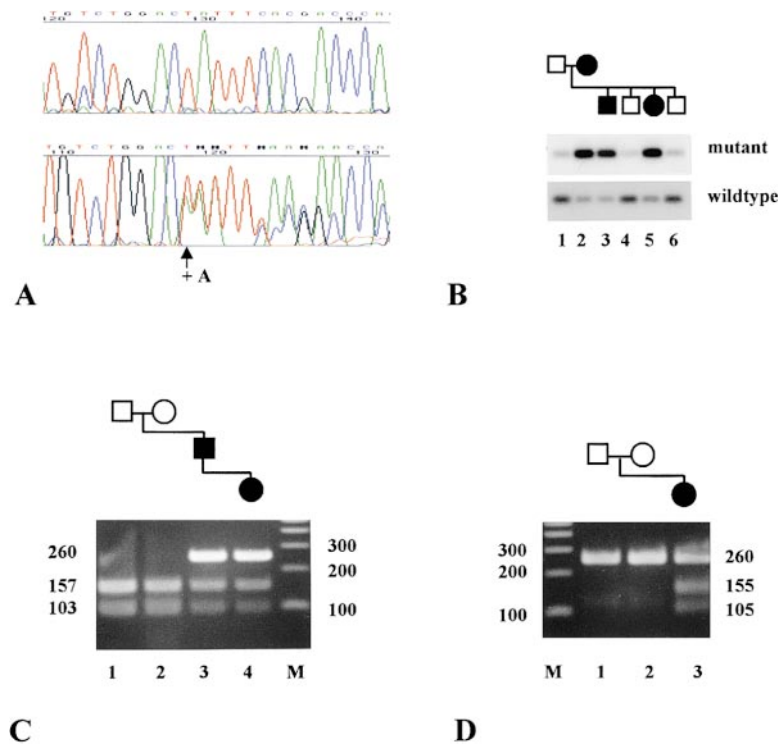


Figure 3. Segregation of p63 Mutations in Families with EEC Syndrome

(A) Frameshift mutation in family Nij-4. Partial sequence of a PCR amplicon containing exon 13 derived from patient Nij-1 (bottom) and her healthy mother (top). The extra adenosine in one of the alleles of the patient is not present in her father's (not shown) and mother's DNA. (B) ASO hybridization of the Arg279His mutation in family SLC-1. PCR fragments derived from exon 7 were electrophoresed in a 2% agarose and transferred to two separate nylon filters by Southern blotting. Each filter was hybridized with a ^{32}P -labeled oligonucleotide, with either a complete match to the wild-type allele (5'-ATG AAC CGC CGT CCA ATT-3') or to the mutant allele (5'-ATG AAC CAC CGT CCA ATT-3'). (C) Segregation of the Arg304Trp mutation in family Nij-1. The 260 bp PCR fragment containing exon 8 was digested with HpaII. The wild-type product is cleaved into fragments of 157 and 103 bp. Due to the mutation the HpaII site is lost, resulting in partial digestion of PCR fragments derived from affected individuals. Note that the mutation has occurred *de novo* in the germline of one of the grandparents. (D) Segregation of the Cys306Arg mutation in family Nij-2. The 260 bp PCR fragment containing exon 8 was digested with BamHI, which gives rise to products of 155 and 105 bp for the mutant allele, while the wild-type allele is not digested. Note that the mutation has occurred *de novo* in the germline of one of the parents.

showing a substitution by tryptophan and one by glutamine. In patient Nij-1 a change of C to T at nucleotide position 910 (with respect to the A of the start codon) results in a missense mutation Arg304Trp. Another missense mutation Cys306Arg was found in patient Nij-2. Both mutations are located in exon 8 of the *p63* gene, which encodes a core element of the DNA-binding domain. Two other missense mutations, Ser272Asn and Arg279His, are located in exon 7. Finally, an insertion of one nucleotide (1572insA) was detected in exon 13 of patient Nij-4, resulting in a frameshift at codon 525 (tyrosine) and a premature stop codon in the same exon (Figure 3A).

In at least five families, the mutation is *de novo*: family Nij-1 (Arg304Trp), Nij-2 (Cys306Arg), Nij-3 and Lei-1 (both Arg204Trp), and Nij-4 (frameshift) (Figure 3 and data not shown). In two of the families that map to chromosome 3q27, Leu-1 and SLC-1, cosegregation of the mutation and the disease was observed (Figure 3B and data not shown). For all mutations the mutant allele was not present in 100 investigated control chromosomes. A comparison between the DNA-binding domains of p53, p63, and p73 demonstrated that all mutated amino acids are strictly conserved (Figure 2B). These data confirm that the *p63* sequence changes are causative mutations for EEC syndrome.

We have not yet identified mutations in the LMS family nor in several EEC syndrome families mapping to 3q27. Most likely, these mutations reside in other parts of the *p63* gene not analyzed here, including exons 1 to 4 or 15.

Protein Modeling Predicts an Impairment of DNA Binding due to p63 Mutations

To obtain a structural context for the mutations described here, we built a model of the p63 DNA-binding domain based on the known structure of its homolog, p53 (Chothia and Lesk, 1986; Sander and Schneider, 1991; Cho et al., 1994; Chinea et al., 1995). According to this model, the p53 and p63 DNA-binding domains assume a similar loop-sheet-helix motif and two large loops that make up the DNA-binding surface of the protein (Figure 4). This model is supported by the fact that p53 and p63 bind to the same DNA motifs (Yang et al., 1998). All amino acids of p53 that directly contact the DNA are conserved in p63, and therefore are predicted to have similar functions (Figure 4). Three of the five positions where amino acid changes cause EEC syndrome are directly implicated in DNA binding. The serine at position 272 (241 in p53) makes a hydrogen bond with a phosphate in the DNA backbone, which is lost upon replacement of this residue by asparagine. The arginine at position 304 (273 in p53) contacts a backbone phosphate. This contact is abrogated by the mutation to tryptophan, which in addition can impose steric hindrance on the DNA binding. Arginine 279 (248 in p53) reaches into the minor groove of the DNA where it contacts nucleotides of adjacent pentamers of the consensus sequence PuPuPuC(A/T) that is required for p53-specific DNA recognition. The amino acid substitutions at the two other positions, arginine 204 and cysteine 306, are predicted to diminish the DNA binding capacity of p63 through structural deformation of the protein.

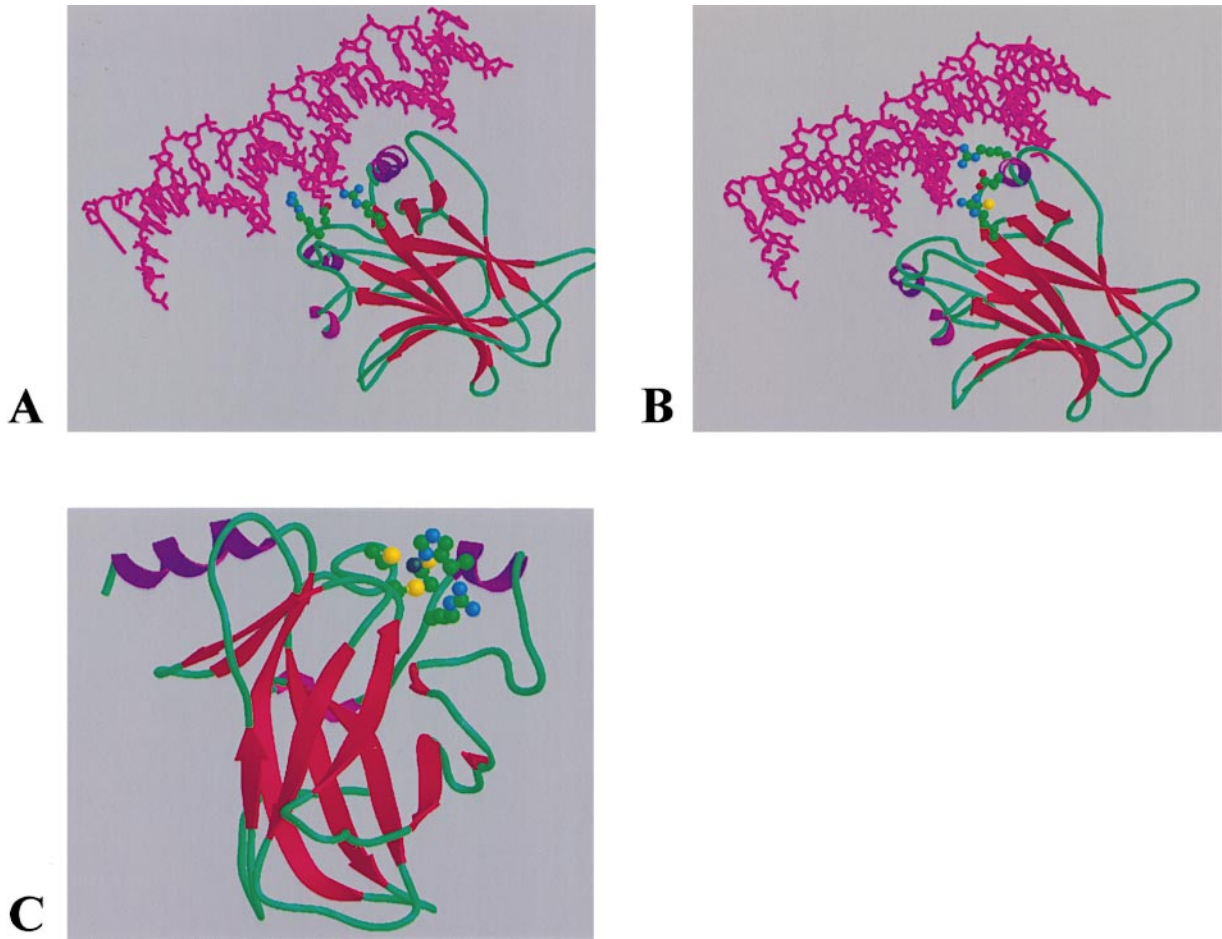


Figure 4. Modeling of the DNA-Binding Domain of p63

In all panels DNA is represented as a purple stick model. Protein is shown as a ribbon model with red strands, blue helices, and green turns and loops. The side chains of interesting residues are shown as ball-and-stick models (C = green; N = blue; O = red; S = yellow; Zn = black).

(A) The protein-DNA complex viewed along the carboxy-terminal helix of the DNA-binding domain (Helix H2 in p53; Cho et al., 1994). From left to right are shown Arg279 (248 in p53), Ser272 (241), and Arg304 (273).

(B) As in (A). Top to bottom are shown Arg311 (280), Asp312 (281), Cys306 (275), and Arg304 (273).

(C) Arg204 (175) is shown just below the Zn-binding site consisting of Cys205 (176), Cys269 (238), Cys273 (242), and His208 (179).

Cys306 (275 in p53) reaches inside the protein where it is located underneath the aspartate at position 312. Asp312 plays an important role in the positioning of the p63 DNA-binding surface by forming salt bridges with Arg304 and Arg311. The Cys306Arg mutation will disrupt the proper contacts between these two arginines and the DNA by destabilizing the Asp312. In p53, the arginine (175) that corresponds to Arg204 in p63 has a critical role in stabilizing two loops (L2 and L3; Cho et al., 1994). Cho et al. (1994) cite several lines of evidence that suggest that mutations of this arginine lead to (partly) unfolded protein. The high degree of local similarity between p53 and p63 in this area of the molecule strongly suggests a similar role for Arg204 in p63, and that mutation of this Arg to Trp or Gln will create extensive structural rearrangements. Thus, all missense mutations are predicted to disrupt DNA binding either directly by replacing amino acids that bind to DNA, or indirectly by creating marked changes in the structural conformation of the DNA-binding domain.

p63 Mutations Affect Transactivation and Dominant-Negative Properties

To assess consequences of p63 mutations found in EEC patients on p63 function, we performed transactivation assays with mutant p63 proteins, containing either an amino acid substitution (Cys306Arg) or the frameshift mutation. Individual p63 mutant and control isotypes were assayed in a cell transfection model for their ability to transactivate p53 reporter genes and to suppress p53- and p63-mediated transactivation, respectively. Whereas wild-type TA-p63 γ , like p53, is a potent transactivator of the p53-responsive reporter gene, the TA-p63 γ ^{Cys306Arg} mutant fails to drive expression from this reporter gene (Figure 5A). The absence of transactivation of the TA-p63 γ ^{Cys306Arg} mutant might have been due to trivial explanations such as destabilization or inability to access the nucleus. However, TA-p63 γ ^{Cys306Arg} had a similar nuclear localization as wild-type protein (data not shown), suggesting the more likely possibility that the Cys306Arg mutation affects p63 binding to DNA

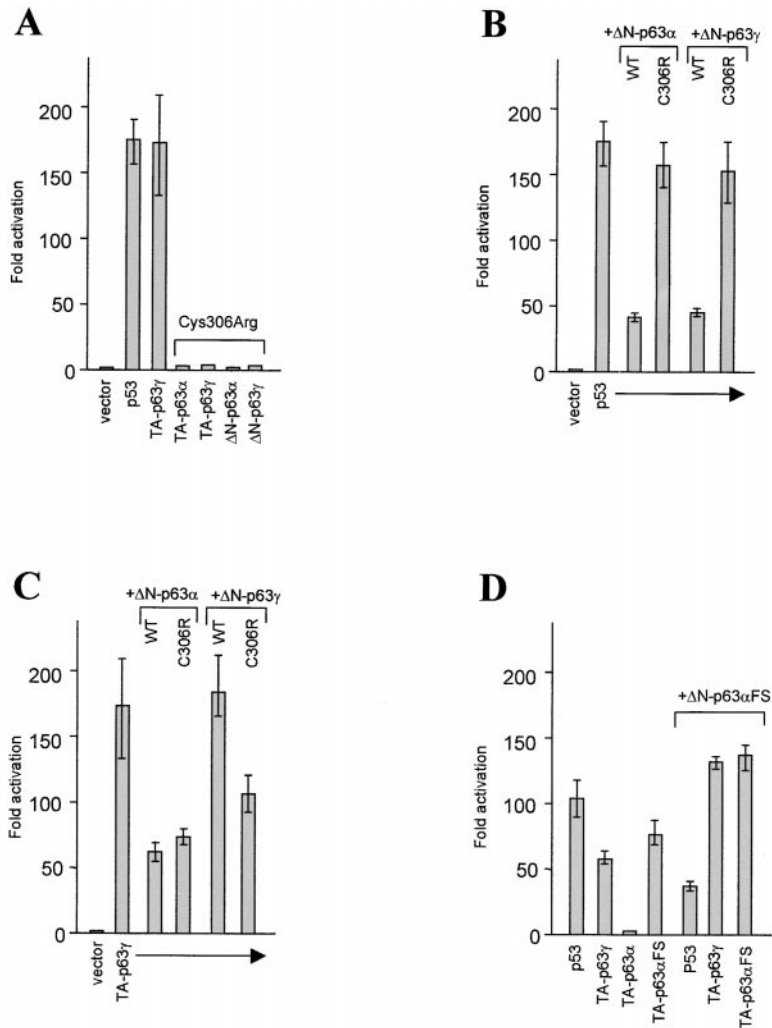


Figure 5. Transactivation of a *p53* Reporter Gene by Wild-Type and Mutant *p53* and *p63* Isoforms

(A) Human Saos-2 cells were transfected as indicated, lysed in detergent lysis buffer 24–36 hr after transfection, and assayed for transactivation using a β -galactosidase reporter gene containing *p53*-binding sites (PG13- β -gal). The transactivation activity of TA-p63 γ is lost due to the Cys306Arg mutation.

(B) Transactivation analysis in Saos-2 cells transfected with wild-type *p53* expression vector, minimal *p53* reporter construct, and either wild-type (WT) or mutant (M) expression vectors at a 1:1 ratio with respect to *p53*, as indicated.

(C) As in (B) except that TA-p63 γ instead of *p53* expression vector was used.

(D) Assessment of the consequences of the frameshift mutation (TA-p63 α FS and Δ N-p63 α FS) for transactivation. Assays were conducted with the indicated combination of constructs as in the above panels.

A constitutive luciferase expression vector (PGL3; Promega) was used in all samples to normalize for transfection efficiency and sample preparation. Error bars indicate SD in triplicate experiments. The relative transactivation at the vertical axis is the degree of stimulation with respect to assays with vector without *p53/p63* sequences.

target sites. Δ N-p63 α , the major *p63* isotype in basal cells of epithelial tissues (Yang et al., 1998), lacks transactivation capabilities against *p53* reporter genes but rather shows remarkable dominant-negative activities toward transactivation of these genes by both *p53* and TA-p63 γ (Yang et al., 1998). We asked whether the Cys306Arg substitution in Δ N-p63 α would affect these dominant-negative activities toward *p53* and TA-p63 γ in the transfected cell model. As expected, wild-type Δ N-p63 α strongly repressed *p53*-induced transactivation of the *p53* reporter gene (Figure 5B), which is likely attributed to effective competition for *p53* DNA target sequences (Yang et al., 1998). In contrast, coexpression of the Δ N-p63 α ^{Cys306Arg} mutant showed no significant effect on the transactivation activity of *p53* (Figure 5B), which indicates that the mutation disrupts the DNA-binding ability of this *p63* isotype. Similar effects toward *p53* transactivation were observed for wild-type and mutant Δ N-p63 γ isotype (Figure 5B). The effects of Δ N-p63 α ^{Cys306Arg} expression on the transactivation functions of TA-p63 γ in this cell model were more complex than toward *p53*. Δ N-p63 α ^{Cys306Arg} was as effective as wild-type Δ N-p63 α in blocking transactivation by TA-p63 γ (Figure 5C). Since Δ N-p63 α ^{Cys306Arg} does not seem to have DNA binding capacity, the observed suppression is likely the result of

the formation of defective heterooligomers between TA-p63 γ and Δ N-p63 α ^{Cys306Arg}. The formation of defective heterooligomeric complexes is also suggested by the effect of mutant Δ N-p63 γ toward TA-p63 γ transactivation. Whereas wild-type Δ N-p63 γ slightly stimulates rather than suppresses transactivation by TA-p63 γ , repression of transactivation is brought about by Δ N-p63 γ ^{Cys306Arg}. It is likely that the ability of heterooligomer formation between mutant and wild-type *p63* isoforms underlies the dominant nature of the *p63* missense mutations in EEC syndrome.

We next investigated whether the frameshift mutation had similar *trans*-dominant effects on transactivation. While TA-p63 α normally lacks transactivation activity, its truncated derivative, TA-p63 α FS, is a strong activator of reporter gene expression (Figure 5D). Thus, the TA-p63 α FS mutant has not only maintained its DNA binding capacity but has also acquired transactivation activity compared to TA-p63 α . TA-p63 α FS lacks almost half of the carboxy-terminal α tail of TA-p63 α , which is completely absent in TA-p63 γ . Apparently, the α tail, or more specifically the domain that is encoded downstream of the nucleotide insertion, confers an autoinhibitory effect on *p63* transactivation. We then asked how the truncation of the α tail would affect the suppressive activities

toward p53 and TA-p63 γ transactivation. In the cotransfection assays, Δ N-p63 α FS suppressed p53-mediated transactivation, which reflects the retained DNA binding capacity of this mutant isotype. Cotransfection of Δ N-p63 α FS with either TA-p63 γ or TA-p63 α FS, however, yielded a significantly higher reporter gene expression than in the absence of Δ N-p63 α FS (Figure 5D). Apparently, Δ N-p63 α FS is able to form potent transactivation complexes with the TA-p63 isoforms. A similar, but less pronounced activity was observed for wild-type Δ N-p63 γ in such cotransfection assays (Figures 5B and 5C).

Discussion

p63 Mutations Cause EEC Syndrome

We have demonstrated that mutations in p63 are an important cause of the EEC syndrome. p63 mutations were found in nine unrelated families. Eight of these mutations cause amino acid substitutions. The ninth mutation introduces a frameshift in exon 13 of the p63 gene, and causes a premature termination codon in the same exon. Unequivocal evidence that the mutations are causative for EEC syndrome was provided by the observation that the changes are *de novo* in five of the families. In addition, the missense mutations are predicted to affect the DNA binding capacity of p63, which results in impaired transactivation activity and altered regulation of transactivation. The premature stop codon introduced by the frameshift mutation does not affect the β and γ isoforms of p63, suggesting a major role for mutant p63 α isotype(s) in the pathogenesis of EEC syndrome. After screening 10 exons (5 to 14) of the p63 gene, we have detected mutations in nine of 25 families, indicating that mutations in the p63 gene are a major cause of EEC syndrome.

The localization of the genetic defect in EEC syndrome family Ams-1 to the 3q27 region was unexpected, because in a previous study significant support was obtained for a location on chromosome 19 (Table 1; O'Quinn et al., 1998). It is possible that the linkage detected at one of these loci is spurious. Alternatively, the identification of linkage to two loci may be indicative for the involvement of genes from the corresponding chromosomal regions acting in concert in developmental processes that are disturbed in this family. A gene from chromosome 19 may thus act as a modifier gene by modulating the phenotypic outcome of p63 mutations.

p63 Mutations in EEC Syndrome Correspond to p53 Hot Spot Mutations in Human Tumors

All of the p63 missense mutations in EEC syndrome patients affect the core DNA-binding domain of the protein at amino acid residues that are strictly conserved among the other members of the p53 family (Figure 2; Kaghad et al., 1997; Schmale and Bamberger, 1997; Yang et al., 1998). Within this DNA-binding domain four evolutionary conserved regions can be distinguished, denoted regions II to V, which are critically important for the proper folding of the protein and for creation of the DNA-binding surface (Cho et al., 1994). All of the identified p63 missense mutations are located in regions III, IV, and V, which in p53 harbor the vast majority of

somatic mutations seen in tumors. The p63 mutations found in the EEC patients occur at amino acids that are commonly altered in p53 proteins found in human malignancies (Hollstein et al., 1991; Hainaut et al., 1998; Walker et al., 1999). There is evidence that the high incidence of mutations at these amino acids in p53 is due to a combination of diverse environmental mutagens, that preferentially bind to CpG dinucleotides, and strong positive selection for mutations, especially for those in the DNA-binding domain (Sidransky et al., 1992).

A similar mechanism of positive selection for mutations seems unlikely for p63. Examination of the nucleotide changes in the p63 gene reveals that six of nine mutations are C-to-T transversions at CpG dinucleotides either on the coding (Arg204Trp [3x], Arg304Trp) or on the noncoding strand (Arg204Gln, Arg279His). It thus seems possible that the codons for these amino acids are hot spots for mutations. An alternative explanation would be that mutation of specific residues such as Arg204 leads to the characteristic ectodermal and limb abnormalities seen in EEC syndrome, whereas mutations at other positions could lead to a different phenotype or have no consequences at all. Despite the amino acid homology between p53 and p63, and the ability of p63 to transactivate p53 target genes (Shimada et al., 1999), there is no indication for an increased susceptibility for cancer development in EEC syndrome patients. Further studies in larger numbers of patients and families with EEC and EEC-like phenotypes (such as LMS) may clarify these issues and, eventually, may enable the identification of genotype-phenotype correlations.

p63 Missense Mutations Affect DNA Binding

The p63 structure model indicates that the observed mutations in EEC syndrome patients will partially or completely abolish DNA binding, either because the DNA contacting amino acids are mutated or because of disruption of the structural integrity of the DNA-binding surface. As a consequence of the diminished DNA binding, the transactivation capacity of the mutant protein will also be reduced. Indeed, cell lysates containing the TA-p63 γ isotype with the Cys306Arg mutation showed a total lack of transactivation activity, whereas lysates with the normal TA-p63 γ isotype do activate transcription of a β -gal reporter gene under control of a minimal p53-binding site. Additional evidence that the Cys306Arg mutation results in a loss of DNA binding capacity is provided by the observation that the Δ N-p63 α ^{Cys306Arg} mutant isotype is unable to suppress p53-mediated transactivation, whereas wild-type Δ N-p63 α efficiently competes with p53 for DNA target sites. The frameshift mutation does not have any apparent effect on the DNA binding capacity of p63, but the resulting truncation of the carboxy-terminal domain clearly has an effect on the normal transactivation (see below).

The Dominant Nature of p63 Mutations

Both EEC syndrome and LMS are inherited in a dominant fashion. Since most mutations identified here in EEC syndrome are predicted to lead to amino acid substitutions, several pathogenic mechanisms are possible. It

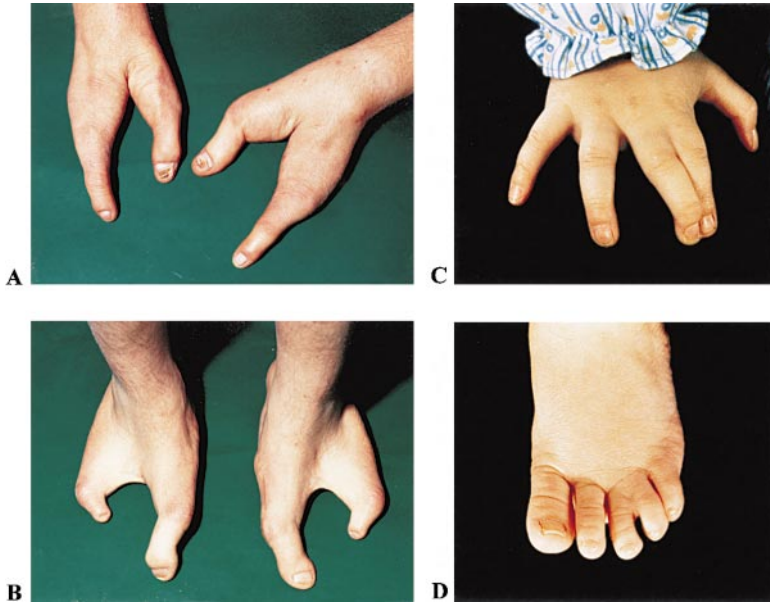


Figure 6. Limb Defects in EEC Syndrome Patients with a Mutation in p63

Typical split-hand with dystrophic nails of the thumbs (A) and typical split-feet (B) from the EEC syndrome patient with a frameshift mutation in exon 13. (C) Cutaneous syndactyly of second and third fingers of the right hand and (D) partial syndactyly of the third and fourth toes of the left foot of the girl with the Arg304Trp mutation (family Nij-1).

cannot be concluded yet which mechanism, haploinsufficiency, dominant-negative, or gain of function, is applicable. Also, the full constellation of symptoms observed in EEC syndrome might be caused by a combination of these mechanisms, as was previously found for several p53 mutations in human tumors (for reviews see Zambetti and Levine, 1993; Ko and Prives, 1996; Levine, 1997). The existence of different p63 isoforms with different properties may complicate the effect of mutations even more.

We feel, however, that haploinsufficiency is not a likely explanation, because patients with germline deletions of chromosome 3q27-qter lack the defining features of EEC/LMS (Chitayat et al., 1996 and references therein). In addition, the p63 homozygous knockout mice that were recently created have severe ectodermal defects and limb anomalies which recall most of the characteristics of EEC/LMS, but heterozygous *wt/-* mice have no obvious phenotypic abnormalities (Mills et al., 1999; Yang et al., 1999). It thus seems that the human p63 mutant proteins found in EEC syndrome exert a dominant-negative or a gain-of-function effect. The acquired transactivation activity of TA-p63 α with the carboxy-terminal truncation could be a gain of function (Figure 5D). However, due to the ability of p63 isoforms to form homo- and heterooligomeric complexes, this mutation, like the Cys306Arg mutation, also has dominant-negative properties in other transactivation assays. Heterooligomeric complex formation underlies the normal suppressive and slightly stimulatory activities of the Δ N-p63 α and Δ N-p63 γ isoforms, respectively, toward TA-p63 γ transactivation (Figure 5C; Yang et al., 1998). Incorporation of mutant isoforms may alter the properties of the entire complex. Indeed, the existence of such compromised complexes is suggested by our finding that mutant Δ N-p63 γ ^{Cys306Arg} has repressive effects toward TA-p63 γ transactivation. Δ N-p63 γ ^{Cys306Arg} has no effect toward transactivation by p53, with which it is unable to complex (Figure 5). Likewise, the normal repressive activity of Δ N-p63 α is converted into a stimulatory effect

toward TA-p63 γ , with which complex formation is possible, while it has retained its suppressive effect on p53-mediated transactivation.

Causal Heterogeneity of Mechanisms Leading to EEC Syndrome

An inherent consequence of the gene structure of p63 is that the mutations observed will affect the function of multiple p63 isoforms. The missense mutations are predicted to affect all six known p63 isoforms, resulting both in a loss of transactivation by TA-p63 γ and to a disruption of repressive properties of other isoforms toward TA-p63 γ . The frameshift mutation, which was found in a patient with a typical EEC syndrome, should not interfere with the production of either the p63 γ or p63 β variants. Consequently, EEC syndrome is not due to a loss of p63 transactivation per se, since the transactivating isoform (TA-p63 γ) is left intact. Instead, the frameshift mutation results in a gain of transactivation activity for the truncated TA-p63 α isoform. The missense and frameshift mutations appear to exhibit divergent effects on the regulation of transcriptional activity of p63 as well. The Cys306Arg missense mutation suppresses the p63-mediated transactivation, whereas the frameshift mutation has a stimulatory effect. The above data suggest that both an increase and a decrease of transactivation by p63 lead to the developmental defects seen in EEC syndrome patients. Of course, this observation is based on transactivation studies with a target gene under control of a p53 response element. The effects in vivo on the transcriptional regulation of the normal p63 target genes may be dependent on additional factors such as the DNA-binding sequence and the nuclear environment.

The EEC Phenotype Resembles that of p63 Knockout Mice

A comparison of the phenotype of p63^{-/-} mice with that of patients who have EEC syndrome shows a strikingly

similar pattern of involved structures. A generalized ectodermal dysplasia is evident in these patients, which manifests as sparse hair, dry skin, pilosebaceous gland dysplasia, lacrimal duct obstruction, and oligodontia. Cleft lip with or without cleft palate occurs in the majority of EEC syndrome patients, which compares to the truncated secondary palate and hypoplastic maxilla and mandibula in *p63*^{-/-} mice (Mills et al., 1999; Yang et al., 1999). There is a wide variety of abnormalities of hand and feet, ranging from syndactyly to a severe defect of the central rays leading to a split hand/split foot malformation (Figure 6). It has been proposed that during evolution similar molecular signaling pathways have been recruited for the formation of structures as diverse as limbs, hair, teeth, and apocrine glands (Thesleff et al., 1995). How these different developmental programs are regulated is largely unknown, but it is of interest that all these structures are affected by heterozygous mutations of *p63*. What these structures have in common is that their development and morphogenesis depends on the signaling between specialized ectodermal cells and the underlying mesoderm. Epithelial-mesenchymal interactions between the apical ectodermal ridge (AER) and the underlying mesenchyme, denoted the progress zone, are required for normal morphogenesis of the limb (Niswander, 1997). Indeed, the limb truncations in *p63*^{-/-} mice seem to be the result of a failure to maintain the AER (Yang et al., 1999).

Clinical variability is one of the hallmarks of EEC syndrome, with clinical expression ranging from severe distal truncations in split hand/split foot malformation (SHFM) to nonpenetrance in obligate heterozygotes who are clinically normal. There are several possible explanations for this extreme variability of symptoms in EEC syndrome. First, stochastic processes may underlie the severity of the various defects. The complexity of interactions between mutant and wild-type isotypes of *p63* could certainly account for this. Secondly, the extent of the defects may be determined by the action of modifier genes and/or environmental factors. A precedent for modifier genes is provided by the *Dactylaplasia* (*Dac*) mouse mutant, which is considered a model for human SHFM3. The *Dac* mouse shows central ray defects of the forelimbs due to excessive cell death of the AER (Seto et al., 1997). The severity of the limb defects in *Dac*^{+/-} mice is dependent on a recessive mutation in a modifier gene, denoted *mdac* (Johnson et al., 1995). By analogy, the various SHFM loci and other unknown genes may act as modifiers of phenotypic expression in EEC/LMS patients. This notion is supported by the possible involvement of two loci, *p63* and a locus on chromosome 19, in one of the EEC families (O'Quinn et al., 1998 and this report). The hypothesis of specific modifier genes can be further pursued by molecular studies of large families with a single *p63* mutation such as the LMS family reported earlier (van Bokhoven et al., 1999).

Experimental Procedures

Linkage Analysis

After obtaining informed consent, genomic DNA from EEC syndrome families was extracted from peripheral blood lymphocytes by a salt extraction procedure (Miller et al. 1988). The DNA concentration

was measured by optical density (OD₂₆₀) and purity checked by determining the OD₂₆₀/OD₂₈₀ ratio. Manual genotyping of microsatellite markers from chromosome 3q27 was carried out as described elsewhere (Kremer et al. 1994). Two-point LOD scores were calculated by the LINKAGE package (Lathrop and Lalouel, 1984). Penetrance was arbitrarily determined at 95% and marker-allele frequencies were estimated by use of the I LINK option. Disease-gene frequency was defined at 0.0001.

Physical Map Construction and Localization of Genes and ESTs

YAC clones from the critical region for LMS/EEC syndrome were selected by using the publicly available resources of the physical mapping project of the Whitehead Institute (<http://www-genome.wi.mit.edu/>; Dib et al., 1996). Yeast cell culturing and DNA isolation was performed as described previously (Green and Olson, 1990). STS markers, ESTs, and genes were physically mapped to these YACs by PCR. Sequences of primers used for mapping of ESTs and genes are available upon request.

Elucidation of the Intron-Exon Boundaries of the *p63* Gene

Primer pairs that were predicted to match neighboring exons of the human *p63* gene were used to amplify the intervening intron from YAC clone 745A12 or total human genomic DNA. Reactions were carried out in a 50 μ l volume containing 20 mM Tris-HCl (pH 8.4), 50 mM KCl, 1.5 mM MgCl₂, 1 mM dNTPs, 250 ng of each primer, and 1.25 unit ExTaq (TaKaRa Biomedicals) under the following conditions: 1 min 94°C, 30 cycles consisting of 5 min 98°C, 30 s 50°C and 15 min 68°C, and 10 min 72°C. PCR products were fractionated by electrophoresis in 2% agarose gels and visualized by staining with ethidium bromide. DNA fragments were excised from the gel and purified with the Qiaquick gel extraction protocol (Qiagen). Sequencing of these fragments was done with the BigDye Terminator chemistry (PE Applied Biosystems) and the use of exon-specific primers. Electrophoresis and analysis was performed on an ABI Prism 377 (PE Applied Biosystems). In case the above exon-bridging strategy was unsuccessful, exon-intron boundaries were determined by direct sequencing with exon-specific primers and PAC DNA as template.

p63 Mutation Analysis

Intron-specific primers were designed that are suitable for amplification of exons 5 to 14 of the *p63* gene: 5F: 5'-GTT GGT TCT CTC CTT CCT TTC-3'; 5R: 5'-GCC CAC AGA ATC TTG ACC TTC-3'; 6F: 5'-CCA CCA ACA TCC TGT TCA TGC-3'; 6R: GTT CTC TCA AGT CTA CTC AGT CC-3'; 7F: 5'-GGG AAG AAC TGA GAA GGA ACA AC-3'; 7R: 5'-CAG CCA CGA TTT CAC TTT GCC-3'; 8F: 5'-GTA GAT CTT CAG GGG ACT TTC-3'; 8R: 5'-CCA ACA TCA GGA GAA GGA TTC-3'; 9F: 5'-ATG CAT TAG TGC TTT AGA AGT G-3'; 9R: 5'-GAA GGT TAA AAT GAA GCA ACC-3'; 10F: 5'-TGA GGA TTG ACC ACA CTT CTA AC-3'; 10R: 5'-CAT CAA TCA CCC TAT TGC TGA TC-3'; 11F: 5'-TGA NCA TCA TTT CCA TGT TTG TC-3'; 11R: 5'-TCA CAG AGT CTT GTC CTA AGC-3'; 12F: 5'-CAA GAT GGA CCA CTG GGA TG-3'; 12R: 5'-GGA CTA TAA CAG TAT CCG CCC-3'; 13F: 5'-CTT ATC TCG CCA ATG CAG TTG G-3'; 13R: 5'-AAC TAC AAG GCG GTT GTC ATC AG-3'; 14F: 5'-GGG AAT GAT AGG ATG CTG TGG-3'; 14R: 5'-AAG ATT AAG CAG GAG TGC TT-3'. PCR reactions were carried out in a 25 μ l volume containing 100 ng genomic DNA, 20 mM Tris-HCl (pH 8.4), 50 mM KCl, 1.5 mM MgCl₂, 0.2 mM dNTPs, 100 ng of each primer, and 1 unit Taq polymerase (GIBCO-BRL), using the following parameters: 1 min 94°C, 2 min 55°C, 1 min 72°C for 35 cycles. The resulting PCR products were directly sequenced as described above.

Sequence alterations were checked in the families of the corresponding patient and in 50 control individuals by allele-specific oligonucleotide (ASO) hybridization or restriction enzyme digestion of PCR products from the relevant exons. ASO hybridization and washing was performed as described by Shuber et al. (1993).

p63 Protein Modeling

A model of the DNA binding domain of *p63* was created by using the modeling methods described by Chinaea et al. (1995) and the

resolved structure of p53 as template (Cho et al., 1994). Sequence alignment and homology modeling were done with the program WHAT IF (Vriend, 1990).

Transactivation Assays

Plasmid DNA from mammalian expression vectors containing the murine p63 sequence under control of a CMV promoter (Yang et al., 1998) was used as template for site-directed mutagenesis using the QuikChange procedure (Stratagene). To create the Cys306Arg mutation we used oligonucleotide 5'-TCC TGG GCA AGC ACG GAT CCG GGC CTC AA-3' and the reverse complement of it. For construction of the frameshift mutation we employed oligonucleotide 5'-CAT CAT GTC TGG ACA TAT TTC ACG ACC CA-3' and its reverse complement. Clones containing the Cys306Arg mutation were selected for by digestion with BamHI, for which a recognition site was created by the mutation. The entire open reading frame of each clone was checked by sequencing. Transactivation assays were conducted as described previously (Yang et al., 1998).

Acknowledgments

We wish to thank the patients and their families for their kind cooperation to this research; Drs. E. Legius, C. de Die-Smulders, C. Schrander-Stumpel, R. J. Gorlin, and G. Gillesen-Kaesbach for providing patient material; S. van de Velde Visser and B. van den Helm for cell culturing; and E. van Beusekom for some of the linkage studies. This work was supported by a grants from the Dutch Society for Scientific Research, grant NWO 901-04-183 (to H. G. B.), the National Institutes of Health (to F. M. and D. A. H.), and by the Shriners Hospitals for Children (to M. B.).

Received July 6, 1999; revised September 13, 1999.

References

Ahmad, M., Abbas, H., Haque, S., and Flatz, G. (1987). X-chromosomally inherited split-hand/split-foot anomaly in a Pakistani kindred. *Hum. Genet.* **75**, 169-173.

Chinea, G., Padron, G., Hooft, R.W.W., Sander, C., and Vriend, G. (1995). The use of position specific rotamers in model building by homology. *Proteins* **23**, 415-421.

Chitayat, D., Babul, R., Silver, M.M., Jay, V., Teshima, I.E., Babyn, P., and Becker, L.E. (1996). Terminal deletion of the long arm of chromosome 3 [46,XX,del(3)(q27->qter)]. *Am. J. Med. Genet.* **67**, 45-48.

Cho, Y., Gorina, S., Jeffrey, P.D., and Pavletich, N.P. (1994). Crystal structure of a p53 tumor suppressor-DNA complex: understanding tumorigenic mutations. *Science* **265**, 346-355.

Chothia, C., and Lesk, A.M. (1986). The relation between the divergence of sequence and structure in proteins. *EMBO J.* **5**, 823-836.

Crackower, M.A., Scherer, S.W., Rommens, J.M., Hui, C.C., Poorkaj, P., Soder, S., Cobben, J.M., Hudgins, L., Evans, J.P., and Tsui, L.C. (1996). Characterization of the split hand/split foot malformation locus SHFM1 at 7q21.3-q22.1 and analysis of a candidate gene for its expression during limb development. *Hum. Mol. Genet.* **5**, 571-579.

Czeizel, A.E., Vitéz, M., Kodaj, I., and Lenz, W. (1993). An epidemiological study of isolated split hand/foot in Hungary, 1975-1984. *J. Med. Genet.* **30**, 593-596.

Dib, C., Faure, S., Fizames, C., Samson, D., Drouot, N., Vignal, A., Millasseau, P., Marc, S., Hazan, J., Seboun, E., et al. (1996). A comprehensive genetic map of the human genome based on 5,264 microsatellites. *Nature* **380**, 152-154.

Evans, J.A., Vitez, M., and Czeizel, A. (1994). Congenital abnormalities associated with limb deficiency defects: a population study based on cases from the Hungarian congenital malformation registry (1975-1984). *Am. J. Med. Genet.* **49**, 52-66.

Gorlin, R.J., Cohen, M.M., Jr., and Levin, L.S. (1990). *Syndromes of the Head and Neck*, 3rd Edition (New York: Oxford University Press).

Green, E.D., and Olson, M.V. (1990). Systematic screening of yeast

artificial chromosome libraries by use of the polymerase chain reaction. *Proc. Natl. Acad. Sci. USA* **87**, 1213-1217.

Hainaut, P., Hernandez, T., Robinson, A., Rodriguez-Tome, P., Flores, T., Hollstein, M., Harris, C.C., and Montesano, R. (1998). IARC database of p53 gene mutations in human tumors and cell lines: updated compilation, revised formats and new visualisation tools. *Nucleic Acids Res.* **26**, 205-213.

Hollstein, M., Sidransky, D., Vogelstein, B., and Harris, C.C. (1991). p53 mutations in human cancers. *Science* **253**, 49-53.

Johnson, K.R., Lane, P.W., Ward-Bailey, P., and Davisson, M.T. (1995). Mapping the mouse Dactylaplasia mutation, Dac, and a gene that controls its expression, mdac. *Genomics* **29**, 457-464.

Kaghad, M., Bonnet, H., Yang, A., Creancier, L., Biscan, J.C., Valent, A., Minty, A., Chalon, P., Lelias, J.M., Dumont, X., et al. (1997). Monoallelically expressed gene related to p53 at 1p36, a region frequently deleted in neuroblastoma and other human cancers. *Cell* **90**, 809-819.

Ko, L.J., and Prives, C. (1996). p53: puzzle and paradigm. *Genes Dev.* **10**, 1054-1072.

Kremer, H., Pinckers, A., van den Helm, B., Deutman, A.F., Ropers, H.H., and Mariman, E.C.M. (1994). Localization of the gene for dominant cystoid macular dystrophy on chromosome 7p. *Hum. Mol. Genet.* **3**, 299-302.

Lathrop, G.M., and Lalouel, J.M. (1984). Easy calculations of LOD scores and genetic risks on small computers. *Am. J. Hum. Genet.* **36**, 460-465.

Levine, A.J. (1997). p53, the cellular gatekeeper for growth and division. *Cell* **88**, 323-331.

Miller, S.A., Dykes, D.D., and Polesky, H.F. (1988). A simple salting out procedure for extracting DNA from human nucleated cells. *Nucleic Acids Res.* **16**, 1215.

Mills, A.A., Zheng, B., Wang, X.-J., Vogel, H., Roop, D.R., and Bradley, A. (1999). *p63* is a *p53* homologue required for limb and epidermal morphogenesis. *Nature* **398**, 708-713.

Niswander, L. (1997). Limb mutants: what can they tell us about normal limb development? *Curr. Opin. Genet. Dev.* **7**, 530-536.

Nunes, M.E., Schutt, G., Kapur, R.P., Luthardt, F., Kukulich, M., Byers, P., and Evans, J.P. (1995). A second autosomal split hand/split foot locus maps to chromosome 10q24-q25. *Hum. Mol. Genet.* **4**, 2165-2170.

O'Quinn, J.R., Hennekam, R.C.M., Jorde, L.B., and Bamshad, M. (1998). Syndromic ectrodactyly with severe limb, ectodermal, urogenital, and palatal defects maps to chromosome 19. *Am. J. Hum. Genet.* **62**, 130-135.

Osada, M., Ohba, M., Kawahara, C., Ishioka, C., Kanamaru, R., Kato, I., Ikawa, Y., Nimura, Y., Nakagawara, A., Obinata, M., and Ikawa, S. (1998). Cloning and functional analysis of human *p57*, which structurally and functionally resembles *p53*. *Nat. Med.* **4**, 839-843.

Raas-Rothschild, A., Manouvrier, S., Gonzales, M., Farriaux, J.P., Lyonnet, S., and Munnich, A. (1996). Refined mapping of a gene for split hand-split foot malformation (SHFM3) on chromosome 10q25. *J. Med. Genet.* **33**, 996-1001.

Roelfsema, N.M., and Cobben, J.M. (1996). The EEC syndrome: a literature study. *Clin. Dysmorphol.* **5**, 115-127.

Sander, C., and Schneider, S. (1991). Database of homology-derived protein structures and the structural meaning of sequence alignment. *Proteins* **9**, 56-68.

Scherer, S.W., Poorkaj, P., Massa, H., Soder, S., Allen, T., Nunes, M., Geshuri, D., Wong, E., Belloni, E., Little, S., et al. (1994). Physical Mapping of the split hand/split foot locus on chromosome 7 and implication in syndromic ectrodactyly. *Hum. Mol. Genet.* **3**, 1345-1354.

Schmale, H., and Bamberger, C.A. (1997). A novel protein with strong homology to the tumor suppressor p53. *Oncogene* **15**, 1363-1367.

Senoo, M., Seki, N., Ohira, M., Sugano, S., Watanabe, M., Tachibana, M., Tanaka, T., Shinkai, Y., and Kato, H. (1998). A second p53-related protein, p73L, with high homology to p73. *Biochem. Biophys. Res. Commun.* **248**, 603-607.

Seto, M.L., Nunes, M.E., Macarthur, C.G., and Cunningham, M.L.

(1997). Pathogenesis of ectrodactyly in the Dactylaplasia mouse: aberrant cell death of the apical ectodermal ridge. *Teratology* 56, 262–270.

Shimada, A., Kato, S., Enjo, K., Osada, M., Ikawa, Y., Kohno, K., Obinata, M., Kanamaru, R., Ikawa, S., and Ishioka, C. (1999). The transcriptional activities of p53 and its homologue p51/p63: similarities and differences. *Cancer Res.* 59, 2781–2786.

Shuber, A.P., Skoletsy, J., Stern, R., and Handelin, B.L. (1993). Efficient 12-mutation testing in the CFTR gene: a general model for complex mutation analysis. *Hum. Mol. Genet.* 2, 153–158.

Sidransky, D., Mikkelsen, T., Schwechheimer, K., Rosenblum, M.L., Cavanee, W., and Vogelstein, B. (1992). Clonal expansion of p53 mutant cells is associated with brain tumour progression. *Nature* 355, 846–847.

Thesleff, I., Vaahtokari, A., and Partanen, A.M. (1995). Regulation of organogenesis: common molecular mechanisms regulating the development of teeth and other organs. *Int. J. Dev. Biol.* 39, 35–50.

Trink, B., Okami, K., Wu, L., Sriuranpong, V., Jen, J., and Sidransky, D. (1998). A new human p53 homologue. *Nat. Med.* 4, 747–748.

van Bokhoven, H., Jung, M., Smits, A.P.T., van Beersum, S., Ruschendorf, F., van Steensel, M., Veenstra, M., Tuerlings, J.H.A.M., Mariman, E.C.M., Brunner, H.G., et al. (1999). Limb mammary syndrome: A new genetic disorder with mammary hypoplasia, ectrodactyly, and other hand/foot anomalies maps to human chromosome 3q27. *Am. J. Hum. Genet.* 64, 538–546.

Vriend, G. (1990). WHAT IF: a molecular modeling and drug design program. *J. Mol. Graph.* 8, 52–56.

Walker, D.R., Bond, J.P., Tarone, R.E., Harris, C.C., Makalowski, W., Boguski, M.S., and Greenblatt, M.S. (1999). Evolutionary conservation and somatic mutation hotspot maps of p53: correlation with p53 protein structural and functional features. *Oncogene* 9, 211–218.

Yang, A., Kaghad, M., Wang, Y., Gillett, E., Fleming, M.D., Dotsch, V., Andrews, N.C., Caput, D., and McKeon, F. (1998). p63, a p53 homolog at 3q27–29, encodes multiple products with transactivating, death-inducing, and dominant-negative activities. *Mol. Cell* 2, 305–316.

Yang, A., Schweitzer, R., Sun, D., Kaghad, M., Walker, N., Bronson, R.T., Tabin, C., Sharpe, A., Caput, D., Crum, C., and McKeon, F. (1999). p63 is essential for regenerative proliferation in limb, craniofacial and epithelial development. *Nature* 398, 714–718.

Zambetti, G.P., and Levine, A.J. (1993). A comparison of the biological activities of wild-type and mutant p53. *FASEB J.* 7, 855–865.